nature medicine

PDGF-BB modulates hematopoiesis and tumor angiogenesis by inducing erythropoietin production in stromal cells

Yuan Xue[1], Sharon Lim[1], Yunlong Yang[1], Zongwei Wang[1], Lasse Dahl Ejby Jensen[1], Eva-Maria Hedlund[1], Patrik Andersson[1], Masakiyo Sasahara[2], Ola Larsson[3], Dagmar Galter[4], Renhai Cao[1], Kayoko Hosaka[1] & Yihai Cao[1,5]

The platelet-derived growth factor (PDGF) signaling system contributes to tumor angiogenesis and vascular remodeling. Here we show in mouse tumor models that PDGF-BB induces erythropoietin (EPO) mRNA and protein expression by targeting stromal and perivascular cells that express PDGF receptor-β (PDGFR-β). Tumor-derived PDGF-BB promoted tumor growth, angiogenesis and extramedullary hematopoiesis at least in part through modulation of EPO expression. Moreover, adenoviral delivery of PDGF-BB to tumor-free mice increased both EPO production and erythropoiesis, as well as protecting from irradiation-induced anemia. At the molecular level, we show that the PDGF-BB–PDGFR-β signaling system activates the EPO promoter, acting in part through transcriptional regulation by the transcription factor Atf3, possibly through its association with two additional transcription factors, c-Jun and Sp1. Our findings suggest that PDGF-BB–induced EPO promotes tumor growth through two mechanisms: first, paracrine stimulation of tumor angiogenesis by direct induction of endothelial cell proliferation, migration, sprouting and tube formation, and second, endocrine stimulation of extramedullary hematopoiesis leading to increased oxygen perfusion and protection against tumor-associated anemia.

Genetic and epigenetic changes in the tumor environment often lead to elevated amounts of a variety of angiogenic factors that switch on an angiogenic tumor phenotype, which is essential for tumor growth, invasion and metastasis[1–4]. For example, expression of vascular endothelial growth factor-A (VEGF-A), PDGF, fibroblast growth factor and angiopoietins are often upregulated in malignant tissues[1,5–10]. Although all of these factors are able to induce tumor neovascularization, they each have specific vascular targets, angiogenic activity and effects on vascular remodeling. For example, VEGF-A primarily targets vascular endothelial cells through binding to VEGFR-1 and VEGFR-2 receptors, which transduce both angiogenic and vascular permeability activities[11]. As a result, the VEGF-induced vasculature is often disorganized, premature and leaky. In contrast, PDGF-BB primarily targets perivascular cells, including pericytes and vascular smooth muscle cells (VSMCs), and recruits these cells to nascent vascular networks[5], promoting vascular maturation and remodeling. These factors may also differentially affect other systems in the body. For example, circulating VEGF has been reported to induce an anemic phenotype in preclinical models[12], whereas here we find that circulating PDGF-BB promotes extramedullary hematopoiesis.

Either alone or collaboratively, these tumor-derived angiogenic factors promote the neovascularization, growth and metastasis of tumors[13]. During malignant progression, the expression patterns and amounts of these angiogenic factors may be altered, with effects on the number, structure, architecture and function of tumor blood vessels. Such vascular alterations can eventually lead to antiangiogenic drug resistance[1,14,15].

The stroma, which constitutes a large portion of various solid tissues and organs, consists of extracellular matrix, vascular cells and mesenchymal cells, including fibroblasts, myofibroblasts and inflammatory cells[15–18]. The tumor stromal compartment contributes to tumor growth by stimulating neovascularization[19]. PDGF-BB (a dimer of the PDGF-B chain), a multifunctional member of the PDGF family, signals through the receptors PDGFR-α and PDGFR-β[20]. PDGF-BB stimulates angiogenesis *in vivo* and in tumors[21–23]. PDGFR-β is a tyrosine kinase receptor localized to the plasma membrane that is abundantly expressed in stromal and mural cells, including fibroblasts, myofibroblasts, pericytes and VSMCs[13,24]. In addition to affecting angiogenesis, PDGF-BB also has marked effects on vascular remodeling, maturation and stability by recruiting pericytes and VSMCs to newly formed angiogenic vessels[24]. Genetic deficiency of PDGF-BB or PDGFR-β leads to early embryonic lethality caused by depletion of pericytes and vascular leakiness[25,26].

EPO, a hormone that stimulates erythropoiesis, is produced in fetal liver and in the kidneys of adults[27]. EPO expression is elevated during tissue hypoxia through activation of the hypoxia-inducible factor-1α (HIF-1α) transcription factor pathway[28]. In addition to stimulation of erythropoiesis, EPO has been reported to promote angiogenesis, vascular stability and endothelial cell survival[29]. Extramedullary hematopoiesis associated with hepatosplenomegaly is often seen in

[1]Department of Microbiology, Tumor and Cell Biology, Karolinska Institute, Stockholm, Sweden. [2]Department of Pathology, Graduate School of Medicine and Pharmaceutical Sciences, University of Toyama, Toyama, Japan. [3]Department of Oncology-Pathology, Karolinska Institute, Stockholm, Sweden. [4]Department of Neuroscience, Karolinska Institute, Stockholm, Sweden. [5]Department of Medicine and Health Sciences, Linköping University, Linköping, Sweden. Correspondence should be addressed to Y.C. (yihai.cao@ki.se).

Received 12 September; accepted 17 October; published online 4 December 2011; doi:10.1038/nm.2575

individuals with various types of cancer[30,31], and high expression of EPO and its receptor is associated with poor survival in these individuals[32]. In this study, we show that PDGF-BB modulates extramedullary hematopoiesis and angiogenesis through activation of EPO production in the stromal compartment.

RESULTS

PDGF-BB in stromal expansion, angiogenesis and tumor growth

We evaluated the ability of PDGF-BB to promote tumor growth, stromal expansion and angiogenesis by overexpressing PDGF-BB in subcutaneous tumors using mouse T241 fibrosarcoma and Lewis lung carcinoma (LLC) cell lines. In T241 tumors, PDGF-BB expression significantly accelerated the tumor growth rate compared to tumors transfected with control vector (hereafter called vector tumors) (**Fig. 1a**). A histological analysis showed that T241 tumors overexpressing PDGF-BB (hereafter called PDGF-BB tumors) contained a high proportion of stroma, which infiltrated the area between tumor cells and cells expressing PDGFR-β (**Fig. 1b**, arrows). We estimated that >50% of the T241 PDGF-BB tumor tissue consisted of stroma. In contrast, vector tumors contained only a modest amount of stromal tissue (**Fig. 1b** and **Supplementary Fig. 1e**). Additionally, T241 PDGF-BB tumors also had a high density of α-smooth muscle actin (α-SMA)-positive structures, which probably correspond to myofibroblasts distributed among the tumor cells (**Fig. 1b**).

We co-stained cells expressing PDGFR-β with several cell-type–specific markers: platelet/endothelial cell adhesion molecule (CD31), isolectinB4 or perfused dextran, marking vascular endothelial cells; chondroitin sulfate proteoglycan 4 (NG2), marking pericytes; and α-SMA, marking VSMCs and myofibroblasts. In addition to the observed stromal tissue expansion in T241 PDGF-BB tumors, the density of the microvessels was significantly greater in PDGF-BB compared to vector tumors, suggesting that PDGF-BB contributes substantially to tumor angiogenesis (**Fig. 1c**,**d**). PDGFR-β was expressed in stromal cells, myofibroblasts and subpopulations of pericytes and VSMCs but was not localized in T241 tumor cells (**Fig. 1c**). A quantitative analysis confirmed that T241 PDGF-BB tumors contained a significantly higher density of PDGFR-β$^+$ cells than did vector tumors (**Fig. 1e**).

Tumor-derived PDGF-BB induces extramedullary hematopoiesis

Necropsy revealed that mice with T241 PDGF-BB tumors showed marked splenomegaly and hepatomegaly compared to mice with vector tumors (**Supplementary Fig. 1a**,**c**), suggesting that tumor-derived PDGF-BB enters the circulation to induce a systemic effect. Circulating amounts of PDGF-BB were significantly higher in mice with T241 PDGF-BB compared to vector tumors (**Fig. 1f**). Notably, a histological analysis showed that hematopoietic foci were often present in the livers of mice with PDGF-BB tumors (**Fig. 1g**) along with a marked expansion of red pulp in the spleen, which eventually became indistinguishable from white pulp (**Fig. 1h**). Similarly, implantation of LLC PDGF-BB tumors resulted in hepatosplenomegaly and increased extramedullary hematopoiesis in the liver and spleen (**Supplementary Fig. 1f**). However, the liver and spleen returned to the sizes observed in healthy mice after surgical removal of established T241 PDGF-BB tumors (**Supplementary Fig. 1c**), showing that the presence of tumors is required to induce hepatosplenomegaly. Similarly, the number of

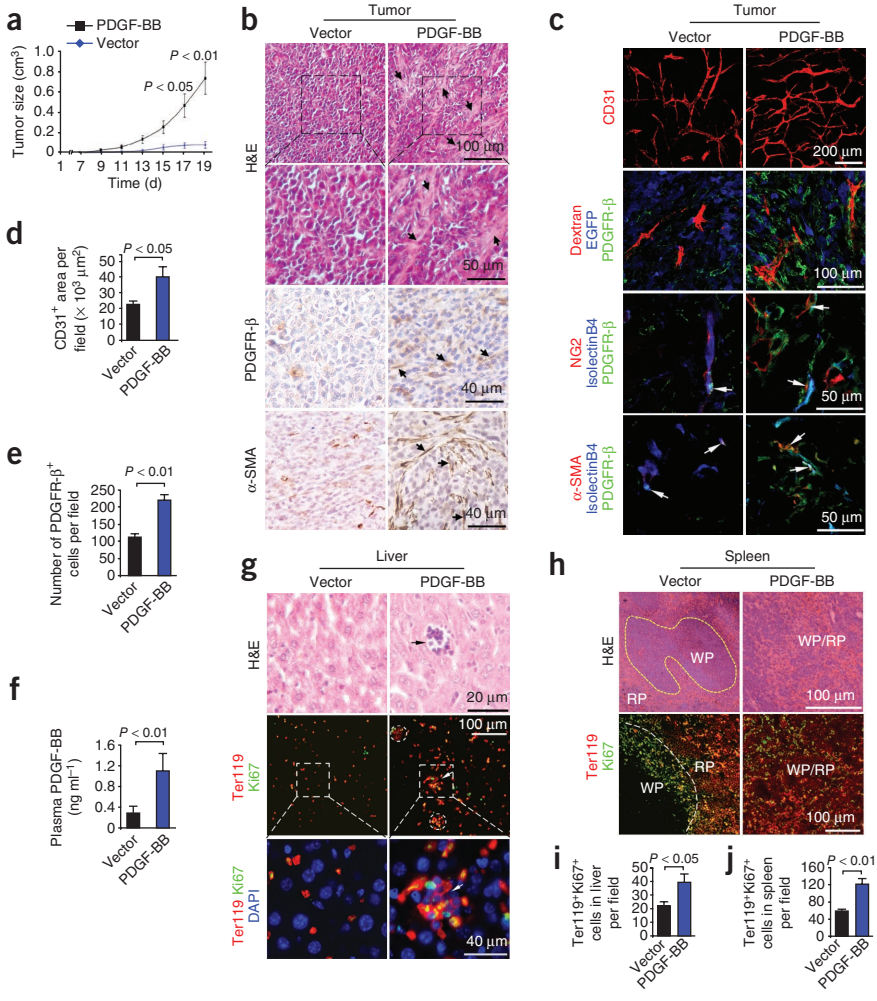

Figure 1 PDGF-BB in stromal expansion, angiogenesis and tumor growth. (**a**) Tumor growth rates of T241 PDGF-BB or vector tumors. (**b**) Tumor tissues were stained with H&E or antibodies specific to PDGFR-β or α-SMA. Arrows point to staining in the tumor stroma and non-tumoral structures. (**c**) Tumor tissues were stained with antibodies specific to CD31, perfused with 2,000 kDa dextran and stained for antibodies specific to PDGFR-β, or were triple stained with isolectinB4, an antibody specific to PDGFR-β and an antibody specific to α-SMA. Tumor cells are labeled with EGFP. (**d**) Quantification of CD31$^+$ vessel area per field (×20 magnification, n = 6–8 per group). (**e**) Quantification of the number of PDGFR-β$^+$ cells per field. (**f**) Plasma concentrations of PDGF-BB in tumor-bearing mice (n = 6–8 per group). (**g**) Liver tissue from mice with PDGF-BB or vector tumors were stained with H&E or triple stained with Ter119, Ki67 and DAPI. Arrows and dashed circles indicate hematopoietic foci. (**h**) Spleen tissue from mice with PDGF-BB or vector tumors were stained with H&E or double stained with Ter119 and Ki67. The dashed lines mark the border between the white pulp (WP) and red pulp (RP). (**i**,**j**) Quantification of Ter119$^+$Ki67$^+$ signals in the liver (**i**) and spleen (**j**) (×20 magnification). Eight micrographs were studied per group, unless otherwise stated (n = 6–8 per group). Data are means ± s.e.m.

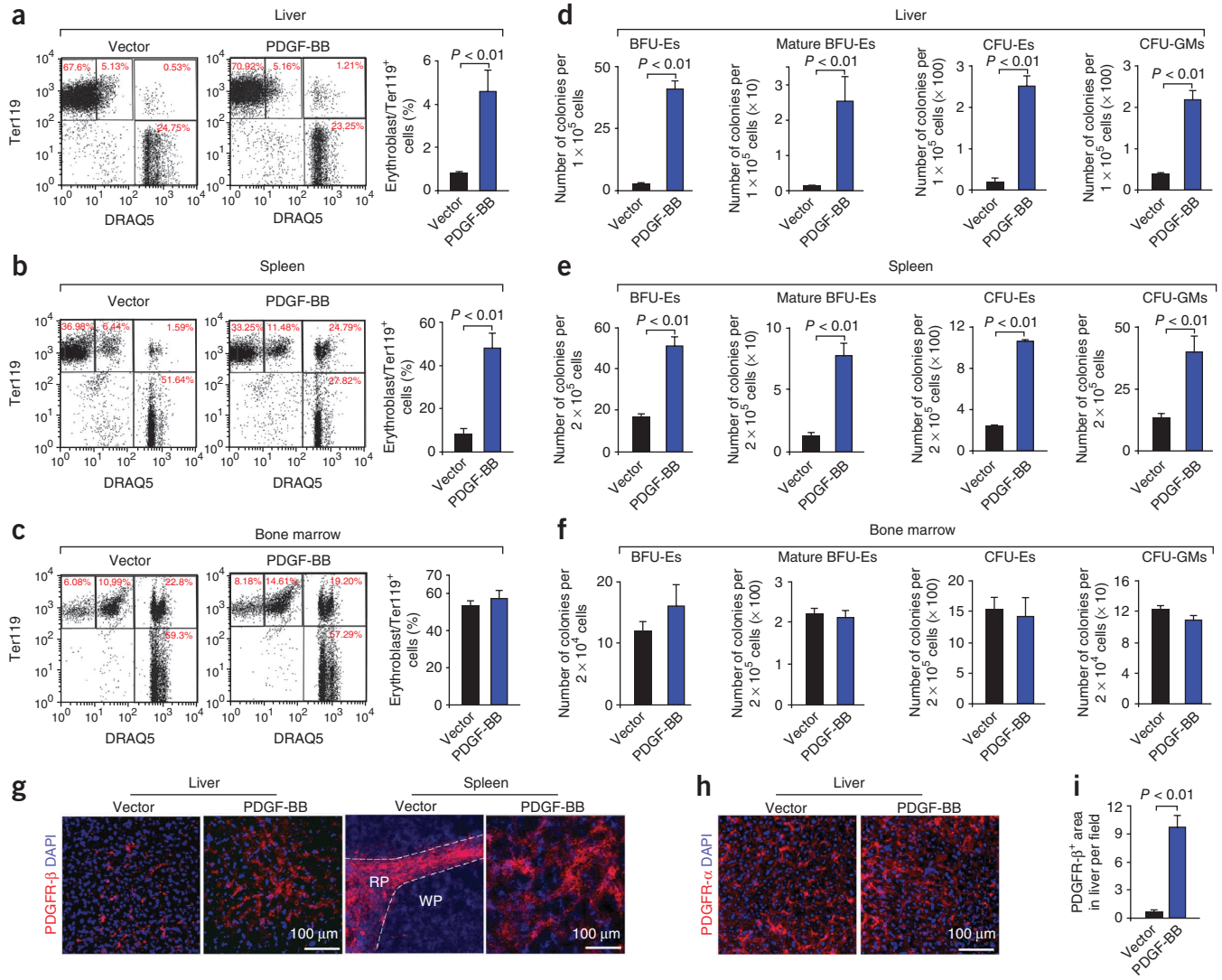

Figure 2 Extramedullary hematopoiesis and expression of PDGFRs in the stromal compartment. (**a**–**c**) Single-cell suspensions from liver (**a**), spleen (**b**) and bone marrow (**c**) of mice with PDGF-BB or vector tumors were double stained with PE-Ter119 and DRAQ5, followed by FACS analysis. The cell population with high Ter119 and DRAQ5 staining represents erythroblasts, the cell population with low Ter119$^+$ and DRAQ5$^+$ staining represents reticulocytes, and the cell population with high Ter119 and no DRAQ5 staining represents erythrocytes. A representative FACS plot from each group and a quantification of the number of erythroblasts compared to the total number of Ter119$^+$ cells is shown ($n = 4$ per group). The numbers in red indicate the percent of the total cell population. (**d**–**f**) Single-cell suspensions from liver (**d**), spleen (**e**) and bone marrow (**f**) from mice with PDGF-BB or vector tumors were cultured with colony-forming assay media to detect BFU-Es, mature BFU-Es, CFU-Es and CFU-GMs. Quantification of the number of colonies is shown ($n = 3$ per group). (**g**,**h**) Liver and spleen tissues from mice with PDGF-BB or vector tumors were double stained with antibody specific to PDGFR-β (**g**, red) or antibody specific to PDGFR-α (**h**, red) and DAPI (blue). (**i**) Quantification of PDGFR-β$^+$ signals in the liver ($n = 8$ per group) (×20 magnification). Data are means ± s.e.m.

hematopoietic foci in the liver and the separation of white pulp and red pulp in the spleen were also normalized after T241 PDGF-BB tumor removal (**Supplementary Fig. 1b**–**d**). In addition, treatment with imatinib (STI571), a tyrosine kinase inhibitor of PDGFR-β, reversed the hematopoietic phenotype induced by T241 PDGF-BB tumors (**Supplementary Fig. 1b**–**d**).

We next asked whether erythroblasts in hematopoietic foci were actively proliferating. We double immunostained tissue sections from liver and spleen with Ter119 and Ki67 to define the proliferating erythroblast population. Indeed, we found a significantly higher number of Ki67$^+$ proliferating erythroblasts in the hematopoietic foci of livers from mice with T241 PDGF-BB tumors compared to mice with vector tumors (**Fig. 1g**,**i**). We also observed a significant increase of Ter119$^+$Ki67$^+$ hematopoietic populations in the spleens of mice with PDGF-BB tumors (**Fig. 1h**,**j**), indicating that tumor-derived PDGF-BB induces active extramedullary hematopoiesis.

We next carried out a fluorescence-activated cell sorting (FACS) analysis on liver, spleen and bone marrow to further characterize the red blood cell (RBC) precursors present in tumor-bearing mice. FACS analysis showed that the number of DRAQ5$^+$Ter119$^+$ RBC precursors in spleen and liver was significantly increased in mice with T241 PDGF-BB tumors compared to those with vector tumors (**Fig. 2a**,**b**). In contrast, we found no significant difference in the numbers of RBC precursors in bone marrow (**Fig. 2c**).

An immunohistochemical analysis of liver tissue showed that the number of CD45$^+$ myeloid cells (where CD45 is a specific marker

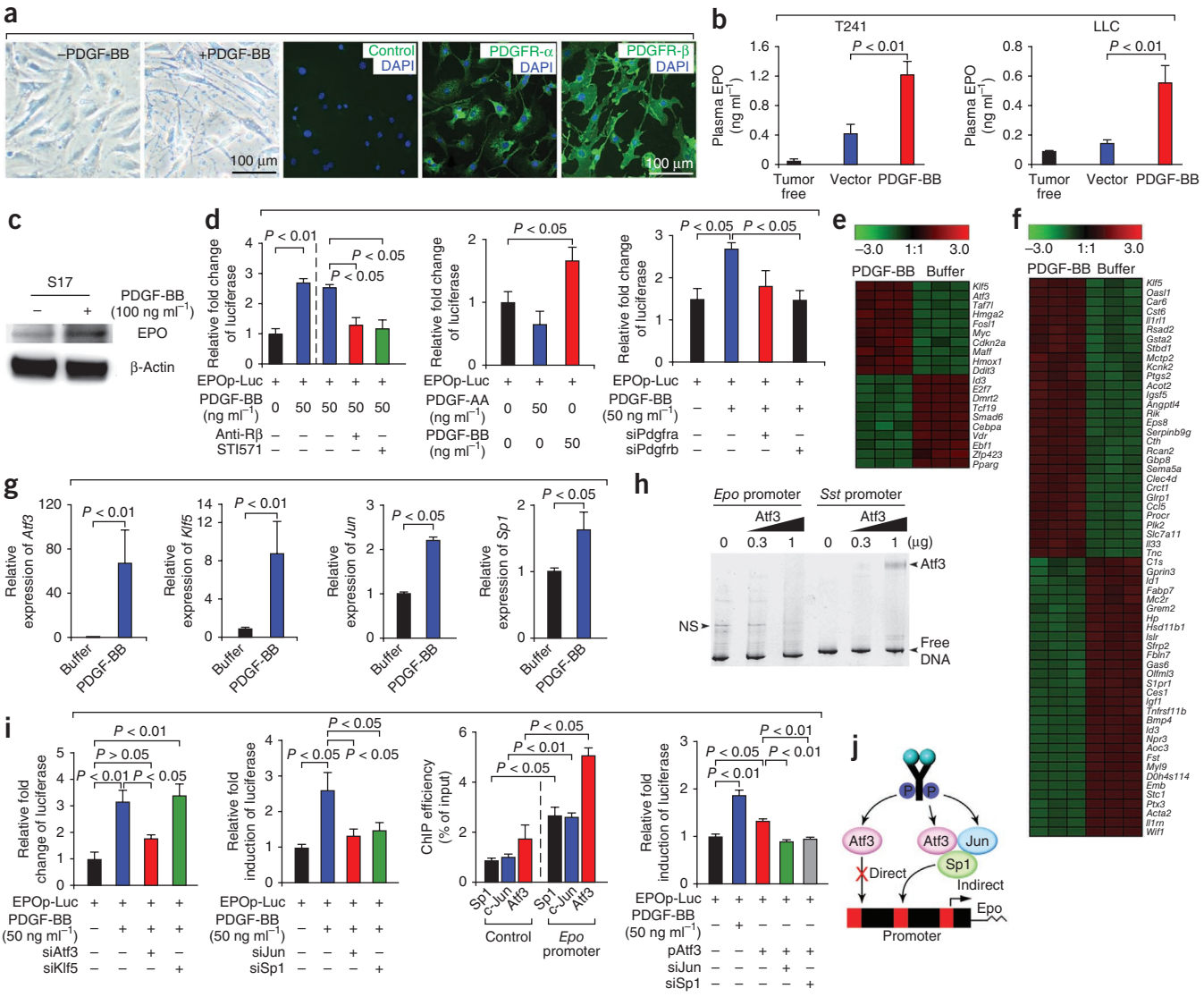

Figure 3 Elevation of plasma EPO concentrations and transcriptional regulation of EPO expression by PDGF-BB. (**a**) Morphology of S17 cells stimulated or not with PDGF-BB that were double stained with DAPI and antibody specific to PDGFR-α or antibody specific to PDGFR-β. (**b**) Plasma concentrations of EPO in tumor-free mice or mice with T241 PDGF-BB, PDGF-BB LLC, or control vector tumors ($n = 6$–8 per group). (**c**) Detection by immunoblotting of EPO protein in S17 cells treated with PDGF-BB or not treated. (**d**) Relative fold induction of *Epo* promoter activity in S17 cells by PDGF-BB treatment in the presence or absence of an antibody specific to PDGFR-β (Anti-Rβ) or STI571 (left); PDGF-AA or PDGF-BB (center); or siRNAs targeting *Pdgfra* (siPdgfra) or *Pdgfrb* (siPdgfrb) (right) ($n = 4$ per group). EPOp-Luc, plasmid construct. (**e**,**f**) Gene array experiments were performed on S17 cells treated with PDGF-BB or buffer ($n = 3$ per group, and expression scale bars are shown on the top). (**e**) Data for the top ten most upregulated and downregulated transcription factor mRNAs. (**f**) Data for the top 30 most upregulated and downregulated mRNAs. (**g**) Expression of *Atf3*, *Klf5*, *Jun* and *Sp1* mRNAs in S17 cells treated with PDGF-BB or buffer quantified by qRT-PCR ($n = 3$ per group). (**h**) EMSA analysis showing a lack of direct binding of Atf3 to the *Epo* promoter. A known Atf3-bound promoter (*Sst*) served as a positive control. NS, nonspecific fragment. (**i**) Left, relative fold induction of *Epo* promoter activity by PDGF-BB in the presence or absence of siRNAs targeting *Atf3* (siAtf3), *Klf5* (siKlf5), *Jun* (siJun) or *Sp1* (siSp1). Middle, detection of the *Epo* promoter binding activity of Sp1, c-Jun and Atf3 transcription factors by ChIP assay. Control, scramble DNA (a nucleotide of the same length with a random sequence). Right, relative fold induction of *Epo* promoter activity by PDGF-BB or by Atf3, and the effects of the indicated siRNAs on Atf3-mediated induction ($n = 3$ per group). pAtf3, plasmid construct. (**j**) A diagram showing possible molecular mechanisms by which PDGF-BB induces EPO expression. See text for details. Data are means ± s.e.m.

of myeloid cells) was significantly ($P < 0.01$) increased in mice with T241 PDGF-BB tumors compared to those with vector tumors (**Supplementary Fig. 2a**,**b**), suggesting that PDGF-BB–induced hematopoiesis is not limited to erythropoiesis. In support of this view, we detected a significantly elevated number of erythroid burst forming units (BFU-Es), mature BFU-Es, erythroid colony forming units (CFU-Es) and granulocyte-macrophage colony-forming units (CFU-GMs) in the liver and spleen of mice with T241 PDGF-BB tumors compared to those with vector tumors (**Fig. 2d**,**e**). In contrast to the liver and spleen, numbers of BFU-Es, mature BFU-Es, CFU-Es and CFU-GMs were unchanged in the bone marrow of mice with T241 PDGF-BB tumors compared to those with vector tumors (**Fig. 2f**), suggesting that PDGF-BB preferentially stimulates extramedullary hematopoiesis rather than bone marrow hematopoiesis.

PDGF-BB protects against tumor-induced anemia

To study the functional consequences of PDGF-BB–induced extramedullary hematopoiesis, we measured RBC numbers, hemoglobin

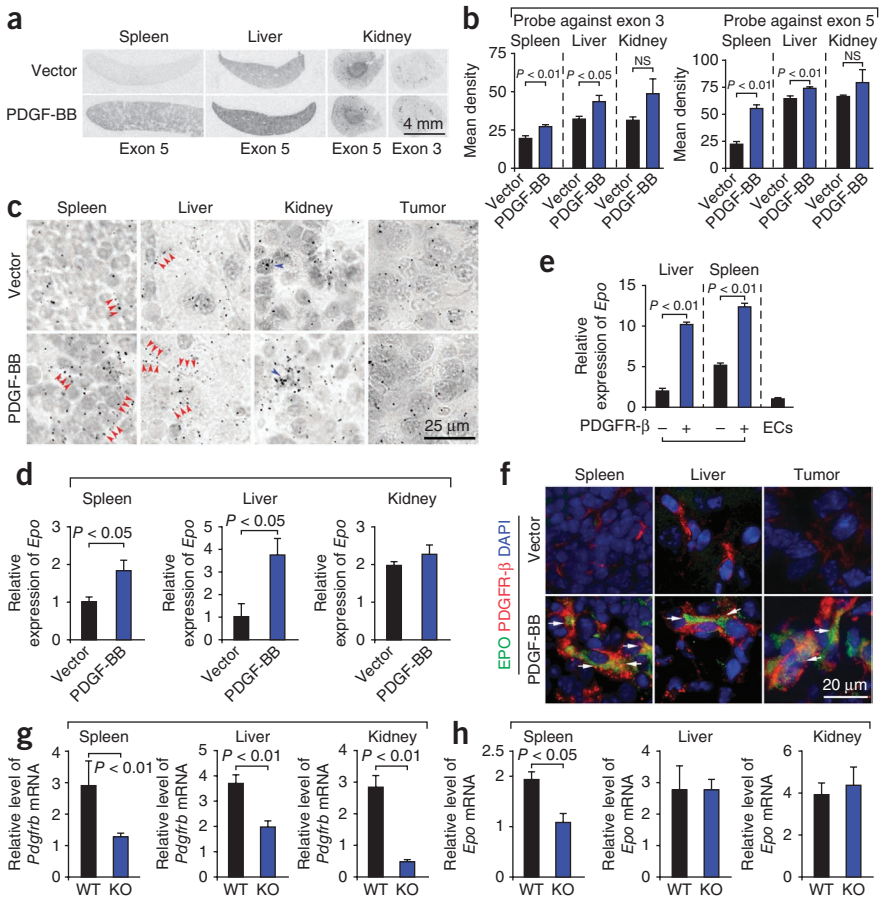

Figure 4 *In vivo* upregulation of *Epo* mRNA by PDGF-BB, co-localization of EPO protein with PDGFR-β$^+$ structures and maintenance of EPO production in spleen by PDGFR-β. (**a**) *In situ* hybridization using probes targeting exon 3 or exon 5 of the mouse *Epo* gene to detect *Epo* mRNA in spleen, liver and kidney from mice with PDGF-BB or vector tumors. (**b**) Quantification of the mean density of positive signals using the exon 3 (left) or exon 5 (right) probe. NS, not significant. $n = 4$ per group. (**c**) *In situ* hybridization at high magnification to detect *Epo* mRNA (using the exon 5 probe) in spleen, liver, kidney and tumors of mice with PDGF-BB or vector tumors. Red arrowheads point to stromal cells positive for *Epo* mRNA; blue arrowheads point to peritubular interstitial cells in kidney positive for *Epo* mRNA. (**d**) Expression of *Epo* mRNA in spleen, liver and kidney of mice with or PDGF-BB or vector tumors determined by qRT-PCR ($n = 4$–6 per group). (**e**) PDGFR-β$^+$ cells in liver and spleen of mice with PDGF-BB tumors were sorted by FACS, and the EPO mRNA level was measured by qRT-PCR. PDGFR-β$^-$ cells isolated from liver and spleen from mice without tumors were used as controls ($n = 3$ per group). ECs, mouse endothelial cells used as a negative control. (**f**) Immunohistochemical detection of EPO (green), PDGFR-β (red) and DAPI (blue) in spleen, liver and tumor of mice with PDGF-BB or vector tumors. Arrows point to EPO$^+$PDGFR-β$^+$ structures. (**g**,**h**) Expression of *Pdgfrb* mRNA (**g**) and *Epo* mRNA (**h**) in spleen, liver and kidney from WT and conditional PDGFR-β knockout (KO) mice ($n = 4$ per group). Data are means ± s.e.m.

concentration and hematocrits in the peripheral blood of tumor-bearing mice. Mice with T241 vector tumors had an anemic phenotype, with significant ($P < 0.05$) decreases in the average value of RBCs, average concentrations of hemoglobin and hematocrit compared to mice without tumors (**Supplementary Table 1**). Notably, mice with T241 PDGF-BB tumors showed significant ($P < 0.05$) improvement in these parameters compared to mice with vector tumors (**Supplementary Table 1**). Moreover, the concentration of white blood cells was increased in mice with T241 PDGF-BB tumors compared to mice with vector tumors. However, the concentration of platelets was not significantly altered in mice with T241 PDGF-BB tumors compared to mice with vector tumors (**Supplementary Table 1**). These findings show that tumor-derived PDGF-BB substantially increases hematocrit, leading to an improvement of tumor-associated anemia.

We next tested whether PDGF-BB–induced erythropoiesis involves the BMP4-mediated stress erythroid response[33]. BMP4 expression was significantly ($P < 0.05$) increased in the liver and spleen of mice with T241 PDGF-BB tumors compared to those with vector tumors (**Supplementary Fig. 2c**,**d**). Additionally, treatment of cell suspensions derived from spleen and liver of mice bearing T241 PDGF-BB tumors with BMP4 and Epo significantly ($P < 0.05$) increased the number of BFU-E colonies compared to treatment with Epo alone, whereas BMP4 did not have this effect on cell suspensions from spleen and liver of mice bearing vector tumors (**Supplementary Fig. 2e**,**f**). These data suggest that BMP4 may, in part, be involved in mediating the PDGF-BB–induced erythroid response.

Expression of PDGFRs in the liver and spleen

In the liver and spleen of mice bearing T241 PDGF-BB tumors, PDGFR-α and PDGFR-β were not expressed in hepatocytes or splenocytes, but were primarily expressed in the stromal compartment (**Fig. 2g–i**). In the liver, PDGFR-β$^+$ signals did not co-localize with albumin, a parenchymal marker expressed by hepatocytes (**Supplementary Fig. 3a**). Rather, PDGFR-β$^+$ signals were co-localized with α-SMA$^+$ (marking VSMCs and myofibroblasts) and NG2$^+$ cells (marking pericytes; **Supplementary Fig. 3b**,**c**). Although the expression of PDGFR-α in the liver did not differ markedly between mice with PDGF-BB tumors and those with vector tumors (**Fig. 2h** and data not shown), the amount of stromal PDGFR-β staining was more than ninefold higher in the liver of mice with PDGF-BB tumors compared to those with vector tumors (**Fig. 2i**). In the spleen, we observed PDGFR-β$^+$ signals exclusively in the red pulp area (**Fig. 2g**), consistent with the idea that PDGFR-β is actively involved in regulating extramedullary hematopoiesis.

We further validated that PDGFR-α and PDGFR-β are expressed in stromal cells using two stromal fibroblast cell lines, MS-5 and S17 (ref. 34). Addition of PDGF-BB to both types of cells resulted in marked morphological changes: the cells became elongated and had spindle-like fibers (**Fig. 3a** and **Supplementary Fig. 3d**). Consistent with the *in vivo* findings, these cells had high levels of PDGFR-α and PDGFR-β expression (**Fig. 3a** and **Supplementary Fig. 3d**).

PDGFR-β–dependent EPO promoter activity in stromal cells

To study the mechanisms underlying PDGF-BB–induced extramedullary hematopoiesis, we measured circulating EPO concentrations. EPO concentrations were increased more than threefold in the plasma

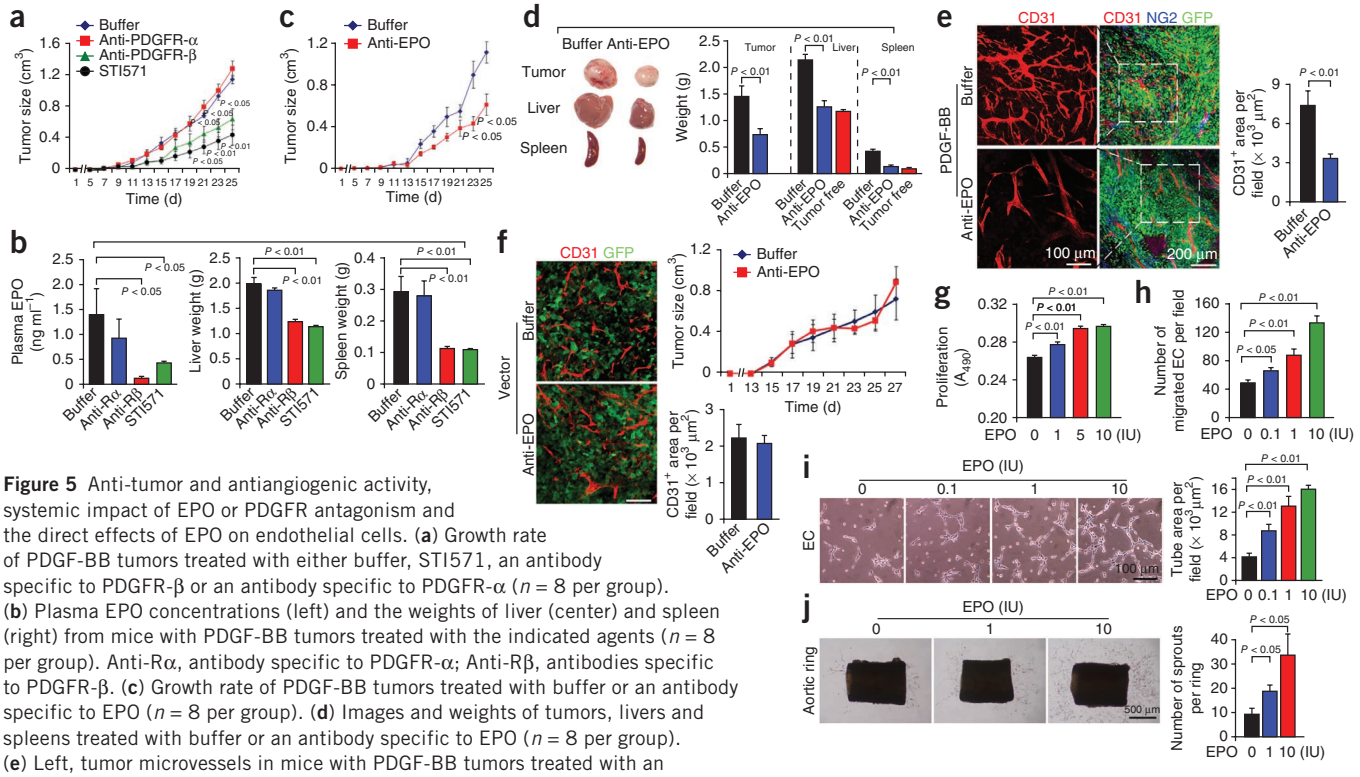

Figure 5 Anti-tumor and antiangiogenic activity, systemic impact of EPO or PDGFR antagonism and the direct effects of EPO on endothelial cells. (**a**) Growth rate of PDGF-BB tumors treated with either buffer, STI571, an antibody specific to PDGFR-β or an antibody specific to PDGFR-α ($n = 8$ per group). (**b**) Plasma EPO concentrations (left) and the weights of liver (center) and spleen (right) from mice with PDGF-BB tumors treated with the indicated agents ($n = 8$ per group). Anti-Rα, antibody specific to PDGFR-α; Anti-Rβ, antibodies specific to PDGFR-β. (**c**) Growth rate of PDGF-BB tumors treated with buffer or an antibody specific to EPO ($n = 8$ per group). (**d**) Images and weights of tumors, livers and spleens treated with buffer or an antibody specific to EPO ($n = 8$ per group). (**e**) Left, tumor microvessels in mice with PDGF-BB tumors treated with an antibody specific to EPO or with buffer as visualized using CD31$^+$ endothelial cell signals (red), NG2$^+$ pericyte signals (blue) and EGFP$^+$ tumor cells (green). Right, quantification of tumor blood vessel area (×20 magnification, $n = 8$ per group). (**f**) Left, tumor microvessels in mice with vector tumors treated with an antibody specific to EPO or with buffer as visualized using CD31$^+$ endothelial cell signals (red) and EGFP$^+$ tumor cells (green). Top right, growth rate of vector tumors treated with an antibody specific to EPO or with buffer. Bottom right, quantification of tumor microvessel area (×20 magnification, $n = 8$ per group). (**g**,**h**) Proliferation (**g**) and migration (**h**) of mouse brain endothelial cells (EC) induced by EPO protein treatment ($n = 6$–8 per group). IU, international unit; A_{490}, absorption at 490 nm. (**i**) Stimulation of endothelial cell tube formation by EPO. Quantification of the vessel-like tube area formed by endothelial cells per field ($n = 8$ per group) (×20 magnification). (**j**) Stimulation of vessel sprouting from mouse aortas by EPO. Quantification of the number of endothelial cell sprouts ($n = 6$ per group). Data are means ± s.e.m.

of mice with T241 or LLC PDGF-BB tumors compared to mice with the corresponding vector tumors (**Fig. 3b**), suggesting that PDGF-BB upregulates EPO expression. Because PDGFRs are expressed in the stromal compartment and in perivascular cells such as pericytes and VSMCs in both the liver and spleen (**Fig. 2g**,**h** and **Supplementary Fig. 3b**,**c**), it is unlikely that PDGF-BB acts directly on hepatocytes or splenocytes to induce EPO expression. PDGF-BB markedly increased the amount of EPO protein in S17 stromal cells, as assessed by immunoblotting using an antibody specific to mouse EPO (**Fig. 3c**).

We next studied the molecular mechanisms by which PDGF-BB induces EPO expression in the stromal compartment. We constructed a full-length mouse EPO promoter upstream of the firefly luciferase reporter gene and transfected this reporter gene construct into S17 stromal cells. Stimulation of the transfected cells with PDGF-BB resulted in a nearly threefold increase of luciferase activity compared to buffer-treated controls (**Fig. 3d**), suggesting that PDGF-BB acts on target cells to activate EPO gene transcription. Treatment with STI571 or a PDGFR-β–specific antibody significantly attenuated transcriptional activation of the EPO promoter (**Fig. 3d**). Stimulation with PDGF-AA, which binds specifically to PDGFR-α, did not significantly induce EPO promoter activity (**Fig. 3d**). To further elucidate the roles of PDGFR-α and PDGFR-β in the transcriptional activation of EPO, we used siRNAs specific to each of the two receptors. Consistent with the data obtained using PDGF-AA, incubation of S17 cells with siRNA targeting PDGFR-β, but not siRNA targeting PDGFR-α, significantly inhibited PDGF-BB–induced EPO promoter activity (**Fig. 3d** and **Supplementary Fig. 3e**). Taken together, these results show that PDGF-BB transcriptionally induces EPO promoter activity through PDGFR-β but not PDGFR-α in stromal cells.

Atf3 mediates PDGF-BB–induced EPO expression

To determine the signaling pathways involved in the regulation of EPO expression by PDGF-BB, we performed an Affymetrix gene array analysis. Gene cluster and principal component analyses showed that the gene expression profiles were highly reproducible in three independent buffer-treated and three independent PDGF-BB–treated samples. We observed both genes that were upregulated and downregulated by PDGF-BB (**Fig. 3e**,**f**). We focused on transcription factors that were upregulated by PDGF-BB to study their potential role in activating EPO promoter activity. Because we identified *Klf5* (encoding the transcription factor Klf5) and *Atf3* (encoding the transcription factor Atf3) as highly upregulated (**Fig. 3e**), we further measured their expression by quantitative real-time PCR (qRT–PCR), which showed an approximately 70-fold increase of *Atf3* and an eightfold increase of *Klf5* in PDGF-BB–stimulated compared to buffer-treated stromal cells (**Fig. 3g**).

To study the effects of Atf3 and Klf5 on the regulation of EPO expression, we designed specific siRNA probes. In stromal cells transfected with the EPO promoter-luciferase reporter construct, *Atf3* siRNA treatment significantly attenuated PDGF-BB–induced reporter activity (**Fig. 3i**), showing that Atf3 mediates the transcriptional upregulation of PDGF-BB–stimulated EPO expression.

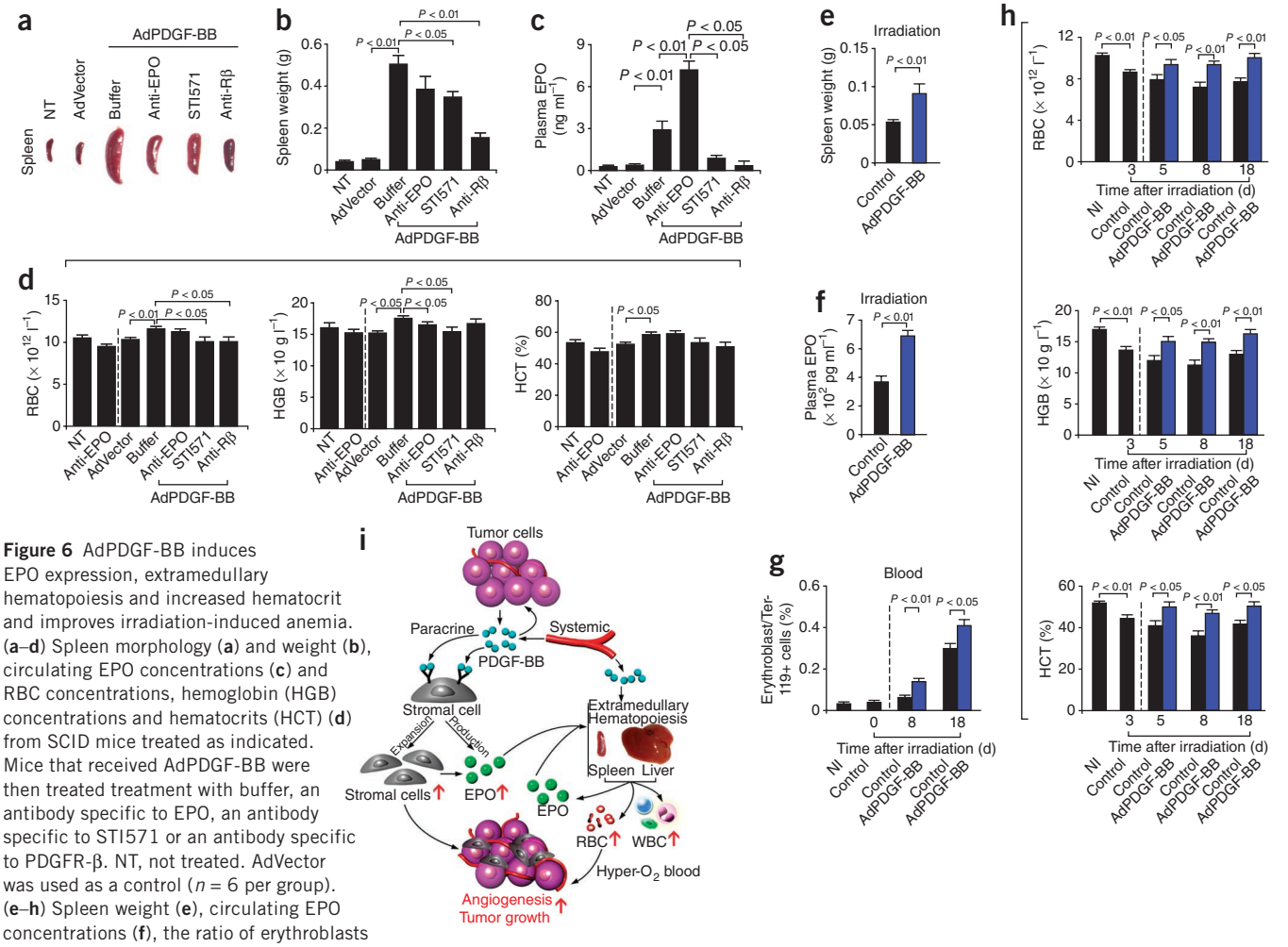

Figure 6 AdPDGF-BB induces EPO expression, extramedullary hematopoiesis and increased hematocrit and improves irradiation-induced anemia. (**a**–**d**) Spleen morphology (**a**) and weight (**b**), circulating EPO concentrations (**c**) and RBC concentrations, hemoglobin (HGB) concentrations and hematocrits (HCT) (**d**) from SCID mice treated as indicated. Mice that received AdPDGF-BB were then treated treatment with buffer, an antibody specific to EPO, an antibody specific to STI571 or an antibody specific to PDGFR-β. NT, not treated. AdVector was used as a control ($n = 6$ per group). (**e**–**h**) Spleen weight (**e**), circulating EPO concentrations (**f**), the ratio of erythroblasts to total erythrocytes (**g**) and RBC concentrations, hemoglobin concentrations and hematocrits (**h**) of sublethally irradiated tumor-free SCID mice that received AdPDGF-BB or control vehicle. The mice were analyzed on days 3, 5, 8 and 18 after irradiation ($n = 4$ per group). NI, non irradiated. Data are means ± s.e.m. (**i**) Mechanisms of tumor-derived PDGF-BB–induced hematopoiesis, tumor growth and angiogenesis. Tumor-derived PDGF-BB enters the circulation (endocrine) to target PDGFR$^+$ stromal cells in organs such as liver and spleen, where PDGF-BB induces EPO expression and activates extramedullary hematopoiesis. Elevated numbers of RBCs may promote tumor growth by decreasing hypoxia in tumors. EPO also protects the host against tumor-associated anemia. In addition to stimulation of hematopoiesis, EPO directly induces tumor angiogenesis. Enhanced hematopoiesis could potentially supply circulating endothelial progenitor cells to the growing tumor vasculature. Hyper-O_2 blood, blood with an increase in oxygen level.

Conversely, treatment with *Klf5* siRNA did not affect the promoter activity of EPO (**Fig. 3i** and **Supplementary Fig. 3e**). Sequence analysis of the EPO promoter region did not reveal any Atf3 consensus-binding sites, suggesting that Atf3 may not act directly on the EPO promoter. Indeed, an electrophoretic mobility shift assay (EMSA) did not provide evidence for direct binding of recombinant Atf3 to the EPO promoter (**Fig. 3h**). Recent studies in neurons have shown that that Sp1 recruits Atf3 and c-Jun to synergistically acquire the capacity to transcriptionally regulate target genes[35]. Notably, the levels of both c-Jun and Sp1 mRNAs were also significantly upregulated in PDGF-BB–treated stromal cells (**Fig. 3g**). Treatment with siRNAs targeting each of these two transcription components led to a significant attenuation of PDGF-BB–induced EPO promoter activity (**Fig. 3i** and **Supplementary Fig. 3e**). Moreover, all three transcription factors bind to the EPO promoter as assessed using chromatin immunoprecipitation (ChIP) assays (**Fig. 3i**), suggesting that these proteins might form a complex. Overexpression of Atf3 alone in S17 stromal cells in the absence of PDGF-BB stimulation led to a substantial increase in EPO promoter activity (**Fig. 3h**). However, Atf3 overexpression alone was not as potent as PDGF-BB treatment in activating the EPO promoter (**Fig. 3i**), suggesting that other proteins might be involved in mediating PDGF-BB signaling. Taken together, these findings provide evidence for an indirect mode of Atf3-dependent EPO expression induced by PDGF-BB (**Fig. 3j**).

PDGF-BB induces stromal EPO expression *in vivo*

Because EPO is almost exclusively produced in the kidneys of adults, we first evaluated EPO mRNA expression in kidneys by *in situ* hybridization. We used two probes, one directed against exon 3 and the other against exon 5 of the mouse *Epo* gene. Kidney EPO mRNA levels were increased only slightly in mice with T241 PDGF-BB tumors compared to those with vector tumors (**Fig. 4a**–**c**). In contrast, *in situ* detection showed that the expression levels of *Epo* mRNA were significantly elevated in both liver and spleen from mice with T241 PDGF-BB tumors compared to those with vector tumors (**Fig. 4a**–**c**). These findings show that upregulation of EPO production

in tumor-bearing animals occurs primarily in extramedullary sites, including the liver and spleen. Consistent with these results, qRT-PCR analysis showed that EPO mRNA levels in the liver and spleen from mice with T241 PDGF-BB tumors were significantly elevated compared to those with vector tumors (**Fig. 4d**). In the kidneys, there was a slight increase in EPO expression, which was not statistically significant.

As shown by immunohistochemistry, EPO^+ cells were present in PDGFR-β^+ stromal tissue of tumors, spleen and liver from mice with T241 PDGF-BB tumors (**Fig. 4**). To further define the cellular source of EPO, we used FACS to sort cells from liver and spleen into PDGFR-β^+ (mice with T241 PDGF-BB tumors) and PDGFR-β^- (mice without tumors) fractions. As expected, the amount of EPO mRNA in the PDGFR-β^+ cell fraction in both liver and spleen was significantly higher than that in the corresponding PDGFR-β^- cell fraction (**Fig. 4e**). In the kidney, EPO-producing cells appeared to correspond to peritubular interstitial cells (PICs), which are known to have high expression of EPO (**Fig. 4a**). In a further immunohistochemical analysis, EPO-producing cells in both tumor and non-tumor tissue of mice with T241 PDGF-BB tumors co-localized with α-SMA, vimentin, CD73, endomucin and desmin (**Supplementary Fig. 4**). In the spleen and liver, co-localization of a subset of EPO^+ signals with α-SMA suggested that VSMCs or myofibroblasts might be involved in EPO production (**Supplementary Fig. 4a**,**b**). In tumor tissue, however, EPO-producing cells were not generally associated with α-SMA or desmin expression (**Supplementary Fig. 4d**). Notably, we detected $CD73^+$ signals (a marker of PICs) in the kidney but not in other tissues (**Supplementary Fig. 4**), indicating that EPO-producing cells in non-kidney tissues do not correspond to PICs.

Taken together, these results further confirm that EPO expression is confined to the stromal compartment in both malignant and non-malignant tissues, and that stromal cells, rather than hepatocytes or splenocytes, are the source of PDGF-BB–induced EPO production. Moreover, EPO-producing cells in various tissues may represent different cell types and may not be directly related to PICs, the cell type that produces EPO in the kidney.

PDGFR-β in EPO maintenance and the role of hypoxia

To study whether the PDGFR-β–mediated signaling system is required for the physiological maintenance of EPO production in various tissues, we carried out an *in vivo* loss-of-function experiment. Global deletion of *Pdgfrb* in adult mice was achieved by crossbreeding mice containing a $Pdgfrb^{flox/flox}$ allele with transgenic mice containing a tamoxifen-inducible Cre construct[36]. Treatment of the resulting mice when they were 4 weeks old with tamoxifen resulted in deletion of *Pdgfrb*[36]. Expression of PDGFR-β mRNA in the spleen, liver and kidney was significantly ($P < 0.01$) reduced in these tamoxifen-treated mice compared to tamoxifen-treated wild-type (WT) mice (**Fig. 4g**). Notably, these mice showed a significant ($P < 0.05$) decrease in EPO mRNA in spleen but not in liver or kidney (**Fig. 4h**), indicating that the PDGFR-β–mediated signaling system is required for the physiological maintenance of EPO expression in the spleen, but not in the liver or kidney. Circulating EPO concentrations in the PDGFR-β–deleted mice and tamoxifen-treated WT mice were similar (**Supplementary Fig. 3f**), supporting the conclusion that the spleen is not a major site for EPO production under physiological conditions.

As it has previously been shown that tissue hypoxia can upregulate EPO expression through activation of the HIF-1α transcription factor pathway[37], we considered the possibility that hypoxia in various tissues and organs in mice with PDGF-BB tumors might contribute to the upregulation of EPO expression. We analyzed tumor and non-tumor tissue sections for tissue hypoxia using a standard hypoxia probe, but observed no clear differences in tumor, liver or spleen tissue between mice with T241 PDGF-BB tumors compared to those with vector tumors (**Supplementary Fig. 5**). This finding suggests that tissue hypoxia does not substantially contribute to PDGF-BB–mediated EPO upregulation, although the role of tissue hypoxia in this regulation warrants further investigation.

EPO in tumor growth, angiogenesis and hematopoiesis

The finding that PDGF-BB stimulates EPO production suggests that EPO might mediate some of the *in vivo* effects of PDGF-BB. A PDGFR-β–specific antibody, but not a PDGFR-α–specific antibody, significantly ($P < 0.05$) attenuated PDGF-BB–stimulated T241 tumor growth (**Fig. 5a**) and tumor neovascularization (**Supplementary Fig. 6a**,**b**). Treatment with STI571 or a PDGFR-β–specific antibody resulted in a reduction of plasma EPO concentrations compared to treatment with buffer (**Fig. 5b**), consistent with our previous results that activation of the PDGFR-β signaling pathway is essential for upregulation of EPO expression in stromal cells. Notably, the PDGFR-β–specific antibody had a more potent inhibitory effect than did STI571, which could be explained by the observation that STI571 had a tendency to increase circulating EPO concentrations in tumor-free mice, as we also saw using other antiangiogenic agents (**Supplementary Fig. 6d**). Because STI571 targets not only PDGFRs but also several other kinases, it is possible that other kinase-mediated pathways, including those mediated by the tyrosine kinase Abl, are involved in the regulation of EPO expression. In addition to inhibiting tumor growth, treatment with STI571 or with PDGFR-β–specific antibody normalized liver and spleen size and weight in mice with PDGF-BB tumors, but treatment with PDGFR-α–specific antibody did not (**Fig. 5b**). These findings show that PDGFR-β is responsible for the accelerated tumor growth rate and hepatosplenomegaly induced by PDGF-BB overexpression.

Similar to the effects of treatment with PDGFR-β–specific antibody, treatment with an antibody specific to mouse EPO[38] also significantly inhibited PDGF-BB tumor growth (**Fig. 5c**,**d**) and angiogenesis (**Fig. 5e**) and prevented PDGF-BB–induced splenomegaly and hepatomegaly (**Fig. 5d**). However, treatment of mice with vector tumors with the EPO-specific antibody did not significantly inhibit tumor growth or angiogenesis (**Fig. 5f**), indicating that the suppression of tumor growth by EPO blockade does not result from global anemia. To further delineate the direct angiogenic activity of EPO, we tested the effects of EPO protein on primary endothelial cells. Treatment with EPO protein significantly stimulated endothelial cell proliferation, cell migration and tube formation in a concentration-dependent manner (**Fig. 5g–i**). Similarly, EPO significantly ($P < 0.05$) induced endothelial cell sprout formation in the aortic ring assay (**Fig. 5j**). These findings support the notion that EPO may act directly on endothelial cells to promote angiogenesis.

Adenoviral PDGF-BB increases EPO levels and hematopoiesis

To exclude the possibility that tumor-derived factors other than PDGF-BB are involved in EPO upregulation and in promoting hematopoiesis, we tested the effects of PDGF-BB delivery alone. We made use of an adenovirus vector expressing PDGF-BB (AdPDGF-BB)[39], which we injected into severe combined immunodeficiency (SCID) mice. We intravenously injected approximately 1×10^8 particles of AdPDGF-BB or an adenovirus vector (AdVector) into each mouse. Because adenoviruses preferentially infect hepatocytes *in vivo*, effects on the liver might be difficult to interpret, and we therefore focused

on splenomegaly as the phenotype of interest. Similar to tumor-derived PDGF-BB, delivery of AdPDGF-BB resulted in splenomegaly (**Fig. 6a**,**b**), a significant increase in the concentration of circulating EPO (**Fig. 6c**), increased concentrations of RBCs and hemoglobin, and an increase in hematocrit (**Fig. 6d**). Notably, administration of STI571 significantly attenuated splenomegaly and reduced the concentrations of RBCs and hemoglobin (**Fig. 6d**), suggesting that PDGFR-mediated upregulation of EPO is responsible for these effects. Similarly, PDGFR-β–specific antibody (**Fig. 6a–d**), but not PDGFR-α–specific antibody (**Supplementary Fig. 7a–c**), markedly reduced splenomegaly, circulating EPO concentrations and the values of RBCs in AdPDGF-BB–treated mice. Circulating PDGF-BB concentrations in the adenovirus model is comparable to those seen in the tumor model (**Supplementary Fig. 7d**). However, treatment with an EPO-specific antibody resulted in only a slight decrease in the concentrations of RBCs and hemoglobin (**Fig. 6d**). These relatively small effects might be due to the long life span of RBCs (approximately 40 d)[40] compared to the duration of treatment (14 d). In support of this view, treatment of WT mice with EPO-specific antibodies did not significantly affect circulating concentrations of RBCs or hemoglobin or hematocrits (**Supplementary Fig. 7h**). Analysis of $DRAQ5^{+}Ter119^{+}$ cell populations by FACS showed that the number of RBC precursors in the spleen was significantly ($P < 0.05$) increased at day 14 after delivery of AdPDGF-BB compared to control mice treated with AdVector (**Supplementary Fig. 7f**), indicating that AdPDGF-BB triggers activation of splenic erythropoiesis. Similar to the results seen in mice with PDGF-BB tumors, the numbers of splenic BFU-Es, mature BFU-Es, CFU-Es and CFU-GMs were significantly ($P < 0.05$) increased in AdPDGF-BB–treated mice compared to those treated with AdVector (**Supplementary Fig. 7e**).

To test whether delivery of AdPDGF-BB could protect against irradiation-induced hematopoietic suppression, we irradiated tumor-free SCID mice at a sublethal dose and then injected them with AdPDGF-BB (**Fig. 6e–h**). We used non-irradiated mice as controls. At day 3 after irradiation, we observed anemia in the irradiated mice: the concentrations of circulating RBCs and hemoglobin and the hematocrits in these mice were significantly decreased compared to those in non-irradiated mice (**Fig. 6h**). Irradiated mice that received AdPDGF-BB showed increased concentrations of circulating RBCs and hemoglobin and hematocrits compared to the control group (**Fig. 6h**). Consistent with the improved numbers of RBCs and hemoglobin concentration, the number of peripheral erythroblasts was also significantly increased in these mice (**Fig. 6g**). A time-course analysis showed that AdPDGF-BB–treated mice recovered faster from irradiation-induced anemia than did control mice (**Fig. 6g**,**h**). Notably, AdPDGF-BB significantly ($P < 0.01$) upregulated the expression of BMP4 in the spleen (**Supplementary Fig. 7g**), which is involved in erythroid radioprotection through a stress-triggered mechanism[33,41,42]. These data suggest that BMP4-dependent stress erythropoiesis is required for the recovery of erythropoiesis induced by AdPDGF-BB in irradiated mice. Taken together, these results show that PDGF-BB administration can protect irradiated mice from anemia, consistent with its ability to stimulate extramedullary hematopoiesis.

DISCUSSION

In this study, we delineate two EPO-mediated mechanisms of PDGF-BB–induced tumor growth (**Fig. 6i**). In a paracrine mechanism, PDGF-BB acts on stromal cells, pericytes or VSMCs that express the PDGF-BB receptor PDGFR-β to expand the stromal compartment and activate EPO expression, leading to enhanced tumor angiogenesis. In an endocrine mechanism, tumor-derived PDGF-BB enters the circulation to induce extramedullary hematopoiesis, which accelerates tumor growth by improving the oxygen and nutrient supply. At the molecular level, we show that the PDGF-BB–PDGFR-β signaling system activates the EPO promoter through induction of the Atf3 transcription factor in association with c-Jun and Sp1. Although our results indicate that the level of tissue hypoxia in tumor, liver and spleen is not altered in mice with tumors overexpressing PDGF-BB compared to those with control tumors, a role for hypoxia in EPO induction cannot be ruled out completely, as hypoxia has previously been reported to regulate Atf3 levels[43].

The finding that stromal cells, pericytes and VSMCs in tumors and other tissues express EPO in response to PDGF-BB is unexpected to us because under physiological conditions, EPO in adults is primarily produced in the kidney. Based on our current work and other previously published findings[29,44,45], it seems that EPO might contribute to tumor angiogenesis through four possible mechanisms (**Fig. 6i**): first, by direct induction of endothelial cell proliferation and migration[29]; second, by increasing vessel stability to further support tumor growth[44]; third, stroma-derived EPO may enter the circulation and stimulate extramedullary hematopoiesis, which would further support tumor growth by improving the nutrient and oxygen supply; and fourth, by stimulating proliferation, differentiation and mobilization of endothelial progenitor cells, which participate in neovascularization[45]. Additionally, the EPO receptor is expressed in certain types of tumor cells and, thus, might act directly on tumor cells.

The circulating concentrations of PDGF-BB (approximately 1 ng ml^{-1}) observed in our preclinical models are similar to those found in individuals with cancer and hence are clinically relevant. For example, in individuals with glioblastoma, the average concentration of plasma PDGF-BB is 880 pg ml^{-1} (ref. 46). Elevated concentrations of plasma PDGF-BB have also been found in individuals with a wide range of other cancers, including lymphoma, sarcomas and epithelial cancers[46,47]. Our preclincial findings suggest that PDGF-BB might also cause systemic effects in individuals with cancer. Indeed, a considerable number of these individuals suffer from hepatomegaly and splenomegaly that have unknown causes[48]. PDGF-BB–induced extramedullary hematopoiesis may have a systemic impact on hematocrit in individuals with cancer. A substantial number of individuals with cancer suffer from bone-marrow–associated anemia, as also seen in our mouse tumor model. We showed that PDGF-BB–induced extramedullary hematopoiesis protects the host against the tumor-associated anemic phenotype. Considering that PDGF-induced elevation of hematocrit may improve the nutrient and oxygen supply in the tumor environment, leading to accelerated tumor growth, the possibility that high hematocrit levels are associated with accelerated tumor growth rates in individuals with cancer warrants further investigation.

Despite the clinical success of targeting the PDGF signaling system in cancer therapy, the underlying mechanisms of such therapy are not well understood. Activation of the PDGF signaling system often occurs as a compensatory switch to alternative angiogenic pathways that lead to resistance to current antiangiogenic therapy. For example, the PDGF signaling pathway may contribute to the acquisition of resistance to VEGF antibody therapy by activating tumor stromal cells[15]. However, treatment with a combination of VEGF and PDGF-specific antibodies produced only modest antitumor activity[49]. Similarly, deletion of host-derived PDGF-BB using a genetic approach did not increase the antitumor activity of a VEGF-specific

antibody[49,50]. Thus, the concept of combination therapy targeting both VEGF and PDGF warrants further preclinical validation.

Our results demonstrate the complex interplay between angiogenic factors in the tumor environment. In light of the protumorigenic effects of EPO, we suggest that elevated EPO levels might confer resistance to the anti-tumor effects of antiangiogenic therapy, such as agents that target PDGF or VEGF pathways[51]. EPO expression can be induced not only by PDGF but also by other factors or mechanisms involving PDGFR-β auto-activation. We anticipate that combinations of PDGF-specific and EPO-specific neutralizing agents would produce greater therapeutic benefits than would single-agent therapy and might be able to overcome the drug resistance associated with therapy using VEGF-specific antibodies. Taken together, our data define a previously unidentified mechanism of PDGF-BB–induced tumor angiogenesis and provide compelling evidence for the key role of EPO in mediating PDGF-BB–induced angiogenesis, tumor growth and hematopoiesis. Although we studied only PDGF-BB, similar regulatory mechanisms might also apply to other members of the PDGF family.

METHODS

Methods and any associated references are available in the online version of the paper at http://www.nature.com/naturemedicine/.

Note: Supplementary information is available on the Nature Medicine website.

ACKNOWLEDGMENTS

We thank J. Nissen and Z. Peng for their technical support. We thank Z. Zhu at ImClone for providing us the antibodies specific to mouse PDGFR-α and PDGFR-β. The MS-5 and S17 cell lines were provided by A. Berardi (Ospedale Bambin Gesu, Italy) and K. Dorshkind (University of California, Los Angeles, California, USA), and the adenoviruses were provided by S. Ylä-Herttuala (University of Kuopio, Kuopio, Finland). This work was supported by the laboratory of Y.C. through research grants from the Swedish Research Council, the Swedish Cancer Foundation, the Karolinska Institute Foundation, the Karolinska Institute distinguished professor award Torsten och Ragnar Söderbergs Stiftelser, a grant from ImClone, the European Union Integrated Project of Metoxia (project number 222741) and the European Research Council advanced grant ANGIOFAT (project number 250021).

AUTHOR CONTRIBUTIONS

Y.C. designed the study and wrote the manuscript. Y.X., S.L., K.H., Z.W., L.D.E.J., R.C. and E.-M.H. performed mouse experiments, as well as histological and immunohistological analyses. Y.X. and S.L. measured the plasma EPO concentrations by ELISA, measured the luciferase activity, performed hematological analyses and performed adenoviral analyses. S.L. performed radiation experiments. Y.X., Z.W. and S.L. cultured stromal cells for *in vitro* assays. Y.Y. performed qRT-PCR, EMSA and ChIP assays. K.H. and Y.Y. performed FACS analyses. K.H. performed colony-forming cell assays and *in vitro* endothelial cell assays. P.A. performed the western blot analysis. S.L. prepared samples for *in situ* hybridization, and D.G. performed *in situ* hybridization assays. Y.X. prepared samples for the microarray assay. Y.X. and O.L. analyzed the microarray data. M.S. provided the PDGFR-β knockout mice for this study.

COMPETING FINANCIAL INTERESTS

The authors declare no competing financial interests.

Published online at http://www.nature.com/naturemedicine/.
Reprints and permissions information is available online at http://www.nature.com/reprints/index.html.

1. Cao, Y. Molecular mechanisms and therapeutic development of angiogenesis inhibitors. *Adv. Cancer Res.* **100**, 113–131 (2008).
2. Carmeliet, P. Angiogenesis in life, disease and medicine. *Nature* **438**, 932–936 (2005).
3. Folkman, J. Angiogenesis: an organizing principle for drug discovery? *Nat. Rev. Drug Discov.* **6**, 273–286 (2007).
4. Kerbel, R.S. Tumor angiogenesis. *N. Engl. J. Med.* **358**, 2039–2049 (2008).
5. Abramsson, A., Lindblom, P. & Betsholtz, C. Endothelial and nonendothelial sources of PDGF-B regulate pericyte recruitment and influence vascular pattern formation in tumors. *J. Clin. Invest.* **112**, 1142–1151 (2003).
6. Ferrara, N. & Kerbel, R.S. Angiogenesis as a therapeutic target. *Nature* **438**, 967–974 (2005).
7. Heldin, C.H., Rubin, K., Pietras, K. & Ostman, A. High interstitial fluid pressure—an obstacle in cancer therapy. *Nat. Rev. Cancer* **4**, 806–813 (2004).
8. Soutter, A.D., Nguyen, M., Watanabe, H. & Folkman, J. Basic fibroblast growth factor secreted by an animal tumor is detectable in urine. *Cancer Res.* **53**, 5297–5299 (1993).
9. Thurston, G. *et al.* Angiopoietin-1 protects the adult vasculature against plasma leakage. *Nat. Med.* **6**, 460–463 (2000).
10. Westermark, B., Nister, M. & Heldin, C.H. Growth factors and oncogenes in human malignant glioma. *Neurol. Clin.* **3**, 785–799 (1985).
11. Cao, Y. Positive and negative modulation of angiogenesis by VEGFR1 ligands. *Sci. Signal.* **2**, re1 (2009).
12. Xue, Y. *et al.* Anti-VEGF agents confer survival advantages to tumor-bearing mice by improving cancer-associated systemic syndrome. *Proc. Natl. Acad. Sci. USA* **105**, 18513–18518 (2008).
13. Nissen, L.J. *et al.* Angiogenic factors FGF2 and PDGF-BB synergistically promote murine tumor neovascularization and metastasis. *J. Clin. Invest.* **117**, 2766–2777 (2007).
14. Bergers, G. & Hanahan, D. Modes of resistance to anti-angiogenic therapy. *Nat. Rev. Cancer* **8**, 592–603 (2008).
15. Crawford, Y. *et al.* PDGF-C mediates the angiogenic and tumorigenic properties of fibroblasts associated with tumors refractory to anti-VEGF treatment. *Cancer Cell* **15**, 21–34 (2009).
16. Bhowmick, N.A. & Moses, H.L. Tumor-stroma interactions. *Curr. Opin. Genet. Dev.* **15**, 97–101 (2005).
17. Kalluri, R. & Zeisberg, M. Fibroblasts in cancer. *Nat. Rev. Cancer* **6**, 392–401 (2006).
18. Pietras, K., Sjoblom, T., Rubin, K., Heldin, C.H. & Ostman, A. PDGF receptors as cancer drug targets. *Cancer Cell* **3**, 439–443 (2003).
19. De Palma, M. *et al.* Tie2 identifies a hematopoietic lineage of proangiogenic monocytes required for tumor vessel formation and a mesenchymal population of pericyte progenitors. *Cancer Cell* **8**, 211–226 (2005).
20. Westermark, B. & Heldin, C.H. Structure and function of platelet-derived growth factor. *Acta Med. Scand. Suppl.* **715**, 19–23 (1987).
21. Cao, R. *et al.* Angiogenesis stimulated by PDGF-CC, a novel member in the PDGF family, involves activation of PDGFR-αα and -αβ receptors. *FASEB J.* **16**, 1575–1583 (2002).
22. Cao, R. *et al.* Angiogenic synergism, vascular stability and improvement of hind-limb ischemia by a combination of PDGF-BB and FGF-2. *Nat. Med.* **9**, 604–613 (2003).
23. Zhang, J. *et al.* Differential roles of PDGFR-α and PDGFR-β in angiogenesis and vessel stability. *FASEB J.* **23**, 153–163 (2009).
24. Lindahl, P., Johansson, B.R., Leveen, P. & Betsholtz, C. Pericyte loss and microaneurysm formation in PDGF-B–deficient mice. *Science* **277**, 242–245 (1997).
25. Lindahl, P. *et al.* Paracrine PDGF-B/PDGF-Rβ signaling controls mesangial cell development in kidney glomeruli. *Development* **125**, 3313–3322 (1998).
26. Soriano, P. Abnormal kidney development and hematological disorders in PDGF β-receptor mutant mice. *Genes Dev.* **8**, 1888–1896 (1994).
27. Moritz, K.M., Lim, G.B. & Wintour, E.M. Developmental regulation of erythropoietin and erythropoiesis. *Am. J. Physiol.* **273**, R1829–R1844 (1997).
28. Sasaki, R. Pleiotropic functions of erythropoietin. *Intern. Med.* **42**, 142–149 (2003).
29. Ribatti, D., Vacca, A., Roccaro, A.M., Crivellato, E. & Presta, M. Erythropoietin as an angiogenic factor. *Eur. J. Clin. Invest.* **33**, 891–896 (2003).
30. Baccarani, M. *et al.* The relevance of extramedullary hemopoiesis to the staging of chronic myeloid leukemia. *Boll. Ist. Sieroter. Milan.* **57**, 257–270 (1978).
31. Kushner, J.P., Lee, G.R., Wintrobe, M.M. & Cartwright, G.E. Idiopathic refractory sideroblastic anemia: clinical and laboratory investigation of 17 patients and review of the literature. *Medicine (Baltimore)* **50**, 139–159 (1971).
32. Saintigny, P. *et al.* Erythropoietin and erythropoietin receptor coexpression is associated with poor survival in stage I non-small cell lung cancer. *Clin. Cancer Res.* **13**, 4825–4831 (2007).
33. Lenox, L.E., Shi, L., Hegde, S. & Paulson, R.F. Extramedullary erythropoiesis in the adult liver requires BMP-4/Smad5-dependent signaling. *Exp. Hematol.* **37**, 549–558 (2009).
34. Nakayama, T., Mutsuga, N. & Tosato, G. Effect of fibroblast growth factor 2 on stromal cell-derived factor 1 production by bone marrow stromal cells and hematopoiesis. *J. Natl. Cancer Inst.* **99**, 223–235 (2007).
35. Kiryu-Seo, S. *et al.* Neuronal injury-inducible gene is synergistically regulated by ATF3, c-Jun, and STAT3 through the interaction with Sp1 in damaged neurons. *J. Biol. Chem.* **283**, 6988–6996 (2008).
36. Tokunaga, A. *et al.* PDGF receptor β is a potent regulator of mesenchymal stromal cell function. *J. Bone Miner. Res.* **23**, 1519–1528 (2008).
37. Grimm, C. *et al.* HIF-1–induced erythropoietin in the hypoxic retina protects against light-induced retinal degeneration. *Nat. Med.* **8**, 718–724 (2002).
38. Hardee, M.E. *et al.* Erythropoietin blockade inhibits the induction of tumor angiogenesis and progression. *PLoS ONE* **2**, e549 (2007).
39. Korpisalo, P. *et al.* Vascular endothelial growth factor-A and platelet-derived growth factor-B combination gene therapy prolongs angiogenic effects via recruitment of interstitial mononuclear cells and paracrine effects rather than improved pericyte coverage of angiogenic vessels. *Circ. Res.* **103**, 1092–1099 (2008).

40. Wang, S., Dale, G.L., Song, P., Viollet, B. & Zou, M.H. AMPKα1 deletion shortens erythrocyte life span in mice: role of oxidative stress. *J. Biol. Chem.* **285**, 19976–19985 (2010).
41. Millot, S. *et al.* Erythropoietin stimulates spleen BMP4-dependent stress erythropoiesis and partially corrects anemia in a mouse model of generalized inflammation. *Blood* **116**, 6072–6081 (2010).
42. Harandi, O.F., Hedge, S., Wu, D.C., McKeone, D. & Paulson, R.F. Murine erythroid short-term radioprotection requires a BMP4-dependent, self-renewing population of stress erythroid progenitors. *J. Clin. Invest.* **120**, 4507–4519 (2010).
43. Ameri, K. *et al.* Induction of activating transcription factor 3 by anoxia is independent of p53 and the hypoxic HIF signalling pathway. *Oncogene* **26**, 284–289 (2007).
44. Chen, J., Connor, K.M., Aderman, C.M. & Smith, L.E. Erythropoietin deficiency decreases vascular stability in mice. *J. Clin. Invest.* **118**, 526–533 (2008).
45. Bahlmann, F.H. *et al.* Erythropoietin regulates endothelial progenitor cells. *Blood* **103**, 921–926 (2004).
46. Kurimoto, M., Nishijima, M., Hirashima, Y., Endo, S. & Takaku, A. Plasma platelet-derived growth factor-B chain is elevated in patients with extensively large brain tumour. *Acta Neurochir. (Wien)* **137**, 182–187 (1995).
47. Leitzel, K. *et al.* Elevated plasma platelet-derived growth factor B-chain levels in cancer patients. *Cancer Res.* **51**, 4149–4154 (1991).
48. Yamaguchi, T. *et al.* Renal cell carcinoma in a patient with Beckwith-Wiedemann syndrome. *Pediatr. Radiol.* **26**, 312–314 (1996).
49. Kuhnert, F. *et al.* Soluble receptor-mediated selective inhibition of VEGFR and PDGFR-β signaling during physiologic and tumor angiogenesis. *Proc. Natl. Acad. Sci. USA* **105**, 10185–10190 (2008).
50. Nisancioglu, M.H., Betsholtz, C. & Genove, G. The absence of pericytes does not increase the sensitivity of tumor vasculature to vascular endothelial growth factor-A blockade. *Cancer Res.* **70**, 5109–5115 (2010).
51. Kirschner, K.M. & Baltensperger, K. Erythropoietin promotes resistance against the Abl tyrosine kinase inhibitor imatinib (STI571) in K562 human leukemia cells. *Mol. Cancer Res.* **1**, 970–980 (2003).

ONLINE METHODS

Mice. Female 6- to 8-week-old C57Bl/6 or SCID mice were bred, acclimated and caged in groups of six or fewer mice at the Department of Microbiology, Tumor and Cell Biology, Karolinska Institute. C57Bl/6 mice were used in all tumor-related experiments, and SCID mice were used for the adenovirus experiments. Mice were anesthetized by injection of a 1:1:2 mixture of hypnorm (Vetapharma), dormicum (Roche) and distilled water before all procedures and killed by a lethal dose of CO_2, which was followed by cervical dislocation. PDGFR-β was depleted in Cre–estrogen receptor transgenic[37] *Pdgfrb*$^{flox/flox}$ mice (University of Toyama, Japan) by oral administration of tamoxifen (Sigma-Aldrich; 9 mg per 40 g of body weight for 5 d consecutively) at 4 weeks of age. *Pdgfrb*$^{flox/flox}$ mice were treated identically and used as controls[36]. After another 4 weeks, the mice were used for experimentation. The mouse studies were approved by the Northern Stockholm Experimental Animal Ethical Committee.

Affymetrix gene array analysis. S17 stromal cells were treated with or without 100 ng ml^{-1} PDGF-BB for 72 h, following which total RNA was extracted with an RNA extraction kit (QIAGEN). Triplicates of each group were used for the gene expression analyses. Samples were labeled using a standard method, as previously described[52]. The labeled samples were analyzed using the Affymetrix Mouse Genome 430 2.0 system. The gene array data have been deposited in the Gene Expression Omnibus, accession number GSE33717. See the **Supplementary Methods** for detailed information.

Immunoblotting. Proteins from total lysates, along with a protein ladder (SM1811, Fermentas), were subjected to SDS-PAGE (NP0301, Invitrogen) followed by wet transferring onto methanol-activated polyvinylidene fluoride membranes (LC2002, Invitrogen). Membranes were blocked at 4 °C with 5% BSA (A8806, Sigma) for 30 min before incubation with a rat antibody specific to mouse EPO (anti-mEPO, R&D Systems) and a monoclonal antibody to mouse β-actin (Cell Signaling) overnight. Membranes were incubated for 45 min with secondary antibodies: an antibody to rat conjugated with horseradish peroxidase Invitrogen) and an antibody to mouse IgG horseradish peroxidase (Dako). Positive signals were visualized using a chemiluminescence detection agent Thermo Scientific).

Mouse tumor experimentation and treatment. Mouse fibrosarcoma T241 or LLC cell lines were transfected to overexpress enhanced green fluorescent protein (EGFP) and PDGF-BB or were transfected with empty vector only carrying EGFP, as previously described[13,53]. Approximately 2×10^5 tumor cells transduced with vector or PDGF-BB were subcutaneously implanted on the dorsal back of each 6- to 8-week-old female C57Bl/6 mouse ($n = 8$ per group), and tumor sizes were measured as previously reported[12]. In the PDGFR blockade experiments, an antibody specific to PDGFR-α (IH3) or an antibody specific to PDGFR-β (2C5) (ImClone) was injected intraperitoneally (i.p.) (0.8 mg per mouse three times per week) into each tumor-bearing mouse ($n = 8$ per group). STI571 (LC Laboratories) was also administrated (1 mg per mouse daily i.p.) to tumor-bearing mice ($n = 8$ per group). Antibody or drug administration began 5 d after tumor implantation. PBS was administered on the same schedule as a control. In some experiments, primary tumors were surgically removed when they reached ~1 cm^3 in size, and the experiments were then continued for an additional 14 d. An antibody specific to EPO (EPO neutralizing antibody, R&D Systems; see **Supplementary Methods**) was i.p. administered to healthy mice or to mice with PDGF-BB or vector tumors ($n = 8$ per group) at a dose of 0.2 mg per kg of body weight three times weekly, with the first administration at day 5 after tumor implantation. In non-tumor bearing mice, STI571 at a dose of 1 mg per mouse was i.p. administered daily for 10 d ($n = 5$). Blood and tissue samples were collected at the end of the experiments.

FACS analysis. Mice ($n = 4$) were killed by administration of a lethal dose of CO_2 at the end of the experiments. Single-cell suspensions were then prepared for FACS analysis. Bone marrow cells were flushed from the femurs and tibias. Spleen and liver tissues were mechanically minced using a 100-μm cell strainer and plunger followed by filtering with a 70-μm strainer. Whole blood was collected by heart puncture using heparinized syringes. Cells were washed with PBS, and 1×10^6 cells from bone marrow, spleen and liver or 25-μl blood samples were incubated in mouse serum containing PBS for 15 min at room temperature (25 °C) followed by incubation with the PE-Ter119 (eBioscience) antibody for 20 min on ice. After washing with PBS, cells were fixed using 1% PFA in PBS containing DRAQ5 (Alexis). Flow analysis was performed by FACSort and CellQuest software (BD Bioscience). PDGFR-β$^+$ cells in liver and spleen of mice with PDGF-BB tumors and PDGFR-β$^-$ cells from mice without tumors were sorted by FACS (see **Supplementary Methods**), and the EPO mRNA level was measured by qRT-PCR.

Immunofluorescent staining. Cryostat tissue sections (9 μm thick) and fixed cultured cells on cover slips were incubated with specific antibodies against CD31, Ki67, Ter119, EPO, PDGFR-α or PDGFR-β using standard immunohistochemical procedures[52]. In the co-localization experiments, several combinations of antibodies, including those to CD31, Ki67, Ter119, EPO, PDGFR-α or PDGFR-β, were simultaneously incubated with the same tissue sample. See **Supplementary Methods** for details about the antibodies and reagents used.

***In situ* hybridization.** *Epo* mRNA was detected in liver, kidney and spleen by *in situ* hybridization with radioactively labeled oligonucleotides. Two different probes were designed to target sequences in exons 3 and 5 (252–301 nt and 464–513 nt, respectively) of the mouse *Epo* gene. Oligonucleotides were labeled with ^{33}P, and sections were hybridized overnight with the radioactive probes, washed and exposed to films. Following exposure in the dark for 3 weeks, radioactive signals were developed and quantified using ImageJ software.

Adenovirus experiments. Adenoviruses were generated as described[39]. All SCID mice received the adenovirus vector (AdVector, 1×10^9 PFU) or adenovirus vector expressing PDGF-BB (AdPDGF-BB, 1×10^8 PFU) in a volume of 100 μl by a single intravenous administration on day 0 or day 3 for irradiation experiments. Mice were killed at day 14 after delivery of the adenovirus. Five mice were used in each group, and age-matched female SCID mice were used as the controls for the hematological analyses.

ELISA. Plasma concentrations of human PDGF-BB or mouse EPO were quantified using sensitive ELISA kits according to the manufacturer's instructions (R&D Systems Inc.)

Statistical analyses. Student's *t* tests (Microsoft Excel) were used to measure statistical differences. $P < 0.05$ was considered statistically significant. For the *in situ* experiment, the statistical analyses were performed using GraphPad Prism 4. Groups were compared using Student's *t* tests.

Additional methods. Detailed methodology is described in the **Supplementary Methods**.

52. Xue, Y. *et al.* Hypoxia-independent angiogenesis in adipose tissues during cold acclimation. *Cell Metab.* **9**, 99–109 (2009).
53. Cao, R. *et al.* PDGF-BB induces intratumoral lymphangiogenesis and promotes lymphatic metastasis. *Cancer Cell* **6**, 333–345 (2004).